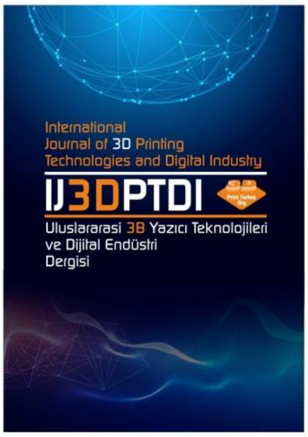

ULUSLARARASI 3B YAZICI TEKNOLOJİLERİ
VE DİJİTAL ENDÜSTRİ DERGİSİ

INTERNATIONAL JOURNAL OF 3D PRINTING
TECHNOLOGIES AND DIGITAL INDUSTRY

ISSN:2602-3350 (Online)
URL: https://dergipark.org.tr/ij3dptdi

FORCE ESTIMATION IN SMART INSOLES USING RANDOMLY PLACED OPTICAL FIBER SENSORS AND MACHINE LEARNING

Yazarlar (Authors): Hüseyin Öztürksoy, Ahmet Özek*, Murat Ekici, Ahmet Çağdaş Seçkin

Bu makaleye şu şekilde atıfta bulunabilirsiniz (To cite to this article): *Ozturksoy H., Ozek A., Ekici M., Seckin A. Ç., "Force Estimation in Smart Insoles Using Randomly Placed Optical Fiber Sensors and Machine Learning" Int. J. of 3D Printing Tech. Dig. Ind., 9(3): 569-578, (2025).*

DOI: 10.46519/ij3dptdi.1784332

Araştırma Makale/ Research Article

Erişim Linki: (To link to this article): https://dergipark.org.tr/en/pub/ij3dptdi/archive

FORCE ESTIMATION IN SMART INSOLES USING RANDOMLY PLACED OPTICAL FIBER SENSORS AND MACHINE LEARNING

Hüseyin Öztürksoy[a], Ahmet Özek[a]*, Murat Ekici[b], Ahmet Çağdaş Seçkin[c]

[a]Pamukkale University, Engineering Faculty, Electrical and Electronics Engineering Department, Turkiye
[b]Dokuz Eylül University, Efes Vocational School, Civil Aviation Transportation Management Program, Turkiye
[c]Aydın Adnan Menderes University, Engineering Faculty, Computer Engineering Department, Turkiye

* *Corresponding Author: ozek@pau.edu.tr*

(**Received:** 15.09.25; **Revised:** 20.11.25; **Accepted:** 24.11.25)

ABSTRACT

This paper presents a smart insole that combines flexible TPU optical fiber sensors with force-sensitive resistors (FSRs) on a 3D-printed TPU base to estimate plantar forces during walking. Three thermoplastic polyurethane optical fibers, illuminated by red lasers and read by light-dependent resistors, were routed in a non-anatomical, irregular ('random') layout and compared against six FSR channels taken as reference targets. Signals were sampled and streamed via an ESP32 microcontroller over Bluetooth. Using a sliding-window approach (20 samples), simple statistical features from the three optical channels were used to train supervised regressors—Gradient Boosting, Adaptive Boosting, and a shallow artificial neural network—to predict each FSR output. Across sensors, models achieved R^2 between 0.865 and 0.951 and mean absolute error (MAE) between 29.0 and 48.9. Adaptive Boosting gave the lowest average MAE and stable R^2, while the artificial neural network reached the highest R^2 for several regions. Results show that accurate force estimation is possible without anatomically precise sensor placement, reducing hardware complexity and cost while keeping performance suitable for gait analysis and wearable health applications.

Keywords: Optical Sensor, TPU Optical Fiber, Machine learning, Smart İnsole

1. INTRODUCTION

The wearable technologies have rapidly spread in recent years thanks to their ability to make real-time measurements under field conditions in both health monitoring and sports performance analytics [1]. Sensor selection is decisive for the success of these systems. Features such as sensitivity, accuracy, repeatability, durability, and cost directly affect the clinical/performance validity of the collected data [2-3]. Flexible and conformable sensors preserve user comfort and the natural flow of mechanical interactions; optical approaches, with immunity to electromagnetic interference and high biocompatibility, fit especially well to wearable settings [4-5].

In this general context, in-shoe insoles allow plantar loading to be monitored during daily life and natural walking, offering a critical platform for both clinical decision support and performance optimization. In people with diabetes, high plantar pressures are known to increase the risk of ulcer development; however, due to time and cost constraints, plantar pressure measurements are not always accessible in routine clinical practice [6]. The role of plantar pressure in identifying foot biomechanics and abnormalities has been shown in many studies, both barefoot and in-shoe [7]. Recent systematic reviews highlight the importance and use cases of in-shoe measurement solutions in high-risk populations such as the diabetic foot [8].

In current insole solutions, the most common approach is distributed resistive and capacitive sensor arrays. However, these architectures are often limited to a small number of sensing regions (e.g., 4–8 zones), rely on predefined layouts, may suffer from calibration and stability issues, and present a challenging cost/complexity trade-off [2, 3, 8]. In this regard, thermoplastic polyurethane (TPU) polymer optical fiber (POF) sensors offer an attractive alternative for wearable insoles thanks to their high flexibility, low Young's modulus, impact resistance, and immunity to electromagnetic interference [4-5]. The literature includes examples where polymer optical fibers are embedded in insoles: with a POF-embedded 3D-printed insole, multi (quasi-distributed) sensing on a single fiber and force/pressure mapping have been demonstrated [5, 9], and fiber-optic insoles have been tested successfully in specific clinical scenarios such as detecting toe walking [10]. More broadly, fiber-optic force sensors are recognised for multi-axial force sensing and safe, EMI-immune measurements in human–machine interaction [11]. In addition, 3D-printing with sensorised fiber/yarn structures enables personalised, low-cost, and scalable production [3], while machine learning has shown high accuracy in distinguishing force and contact patterns [12].

The existing literature supports the feasibility of optical-fiber-based insoles and personalized production via 3D printing, and many studies rely on anatomically structured sensor layouts [3, 9, 12]. This increases manufacturing/ integration complexity and may require redesigning for each user. To our knowledge, there is no reported approach where optical fibers are integrated into the insole with a deliberately non-anatomical, irregular ('random') placement and this layout is interpreted only by machine learning to estimate plantar force with high accuracy [3–5, 8]. This gap offers an opportunity to reduce the number of sensors and hardware costs while preserving clinically/performance-meaningful accuracy. This research challenges the traditional design paradigm by showing that precise force estimation is possible without a highly structured sensor layout. The study has three main contributions:

- We show that non-anatomically routed, randomly placed flexible TPU optical fiber sensors can be used in smart insoles as a valid and effective alternative to traditional FSRs and structured sensor arrays.

- For the first time, we demonstrate that complex optical signals from these non-anatomically distributed ('random') fibers can be interpreted with machine learning algorithms to enable accurate force estimation, removing the need for precise sensor placement to achieve high accuracy.

- We propose a system that reduces the required number of sensors and the total cost while maintaining high accuracy, thus paving the way for more accessible and scalable smart insole technology.

2. MATERIALS AND METHODS

This study aims to measure plantar pressure and bending effects during walking using a multi-sensor insole and to analyze the signals with machine learning. The system combines force-sensitive resistors (FSRs) and soft TPU optical fiber sensors on the same 3D-printed insole. The overall hardware connections and data flow are shown in Figure 1. The instrumented sandal carries a 3D-printed TPU insole with six FSR pads (r1–r6) and three TPU optical fiber channels (o1–o3). Each FSR and each light-dependent resistor (LDR) is connected to an ESP32 microcontroller through a voltage-divider circuit formed by a resistor r. The system is powered by a 5 V rechargeable battery. Analog signals are sampled by the ESP32 and sent wirelessly over Bluetooth to a host computer for recording and machine-learning analysis. Photos from the printing process and the final layout of the insole are given in Figure 2, while the optical sensing principle is illustrated in Figure 3.

A flexible shoe insole was produced by 3D printing using TPU material. The CAD model includes channels and seats to fix the locations of the FSR pads r1–r6 and the optical fibers o1–o3. After printing, six FSRs and three TPU optical fiber lines were placed in these dedicated regions (Figure 2). Prior to integration into the insole, each FSR pad was calibrated individually using a static loading setup with known weights applied via a flat indenter. The resulting voltage–load curves were used to map raw ADC readings to force in Newtons through sensor-specific calibration functions. All FSR values and MAE figures reported in this paper therefore correspond to calibrated forces expressed in N rather than raw sensor counts.

The main hardware components of the system are an ESP32 microcontroller, a 5 V rechargeable battery, six FSRs, three LDRs used as optical receivers, and red laser diodes as optical sources. Each FSR and each LDR is interfaced to an ESP32 analog input via a resistor divider including resistor r, and the resulting voltages are transmitted to the computer over Bluetooth, as summarized in Figure 1.

The flexible optical sensor is a 1.7 mm TPU optical fiber. A red laser diode is coupled to one end of the fiber, and an LDR is mounted at the other end. When the TPU fiber is bent, stretched, or compressed, micro-bends and local stretching increase optical attenuation along the fiber, so part of the light is lost before it reaches the LDR (Figure 3). The LDR converts the received light level into a voltage through the resistor divider. As bending or compression increases, the received light decreases, the LDR resistance increases, and the output voltage changes. These voltage variations are used as indirect measurements of local plantar forces acting on the insole.

All six FSR channels r1–r6 and three optical channels o1–o3 were read by the ESP32 analog inputs and transmitted to the computer over Bluetooth. The data sampling rate was 22 Hz. This rate was chosen as a compromise between temporal resolution, wireless bandwidth, and power consumption when streaming nine analog channels from the ESP32. The walking protocol in this proof-of-concept study consisted of very slow treadmill walking at 1 km/h, so the dominant plantar-force changes occur at low frequencies and our main interest is in quasi-static force envelopes rather than high-frequency impact transients. With this configuration, a sliding window of 20 samples corresponds to approximately 0.9 s of temporal context per feature vector (20/22 s), which is comparable to a gait cycle at the tested speed and was found in the underlying thesis work to maximize R^2 compared with shorter or longer windows.

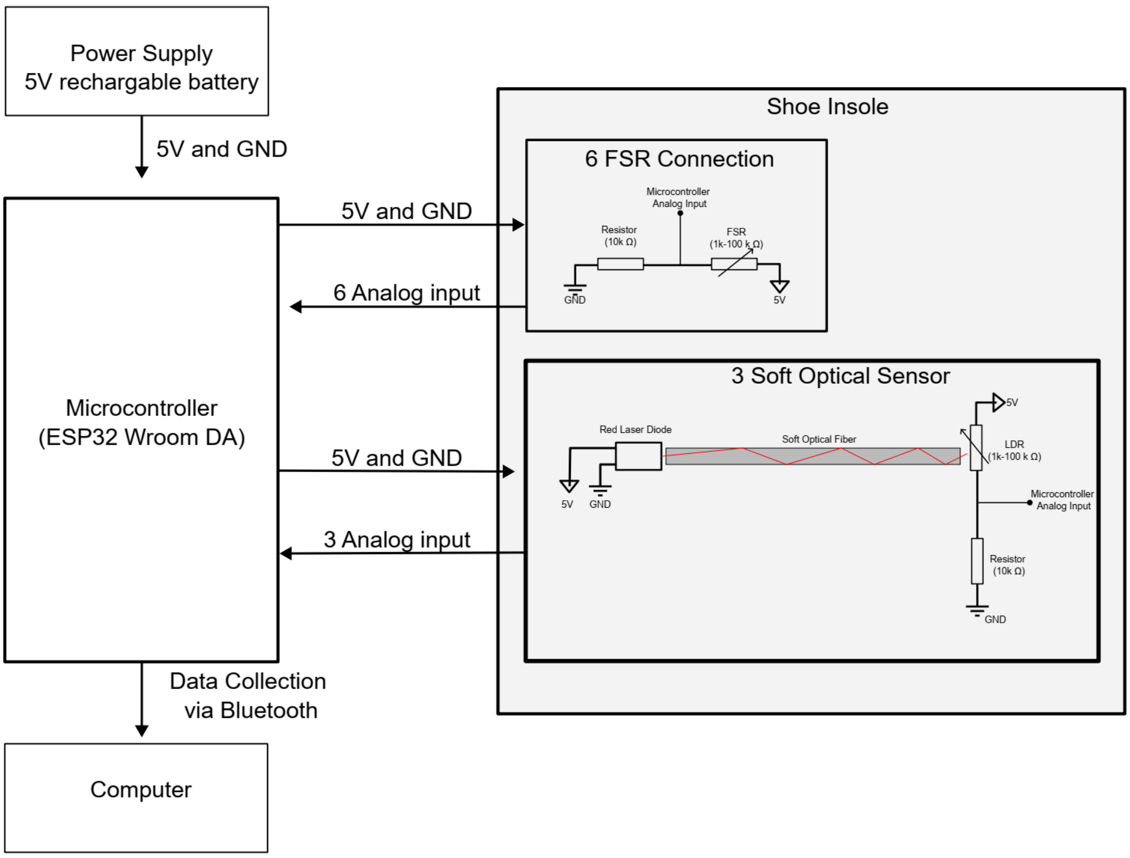

Figure 1: Overview of the smart insole system.

(a) (b) (c)

Figure 2. 3D-printed TPU insole and sensor placement. (a) Top view of the 3D-printed insole shell showing dedicated seats and channels for six FSR pads and three TPU optical fiber paths (b) Intermediate stage of sensor integration. (c) Final prototype with the sensing insole

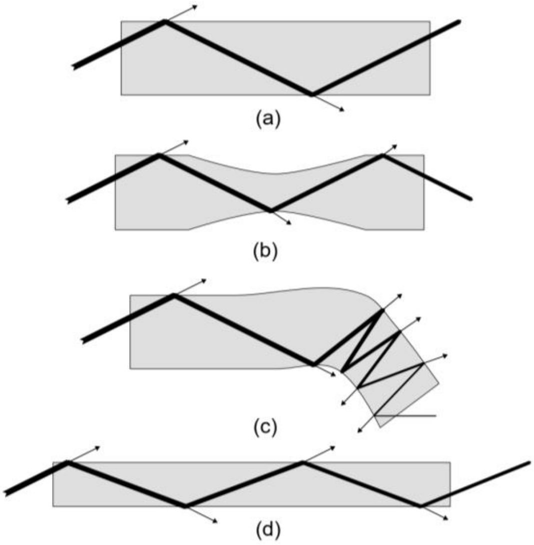

Figure 3: Sensing principle of the TPU optical fiber. Schematic illustration of the flexible TPU fiber and LDR-based receiver under (a) normal, (b) pressed, (c) bent and (d) elongated conditions.

2.1. Machine Learning for Force Estimation

The insole generates nine synchronized analog signals sampled at 22 Hz: three optical channels originating from the TPU optical fiber–laser–LDR assemblies (o1–o3) and six reference force-sensitive resistor channels (r1–r6). All signals are acquired by the ESP32 microcontroller and streamed wirelessly via Bluetooth to a host computer, where they are synchronized and stored for offline processing. The sensing system thus provides two complementary modalities on the same 3D-printed TPU insole: (i) the TPU optical fibers, which form the input modality to be modelled, and (ii) the FSR pads, which provide the reference plantar-force measurements.

Data collection was performed on a treadmill under a controlled protocol. The participant walked for one minute at 1 km/h while wearing the instrumented shoe, producing fully synchronous optical and FSR time series. This protocol targets slow, quasi-static gait patterns aligned with the hardware constraints of the prototype and the 22 Hz sampling regime. The complete data-analysis workflow is summarized in Figure 4, encompassing acquisition, preprocessing, feature extraction, model training, and quantitative evaluation.

Supervised regression was employed to learn the mapping from the three optical channels (o1–o3) to the six FSR channels (r1–r6). Following standard practice for time-series modelling in low-frequency wearable systems, the continuous signals were segmented using a sliding-window transform with 50 % overlap. The window length was fixed at 20 samples, corresponding to approximately 0.9 s of temporal context at 22 Hz. This duration captures the dominant, low-frequency plantar-loading variations of slow gait while balancing temporal resolution and computational cost.

For each window and each optical channel, the following descriptive time-domain features were computed: mean, minimum, maximum, standard deviation, root-mean-square (RMS) value, exponential moving average (EMA), and non-zero sample count. These features form the predictor set. The corresponding FSR values r1–r6 within the same window constitute the regression targets. Separate datasets were constructed for each output channel to support the per-sensor training strategy used throughout the study.

The dataset was split into training and test subsets to quantify generalization performance. Model optimization was conducted on the training portion and performance was assessed on the held-out test data. Three supervised regression families were evaluated:

• Gradient Boosting (GB): An ensemble of decision trees trained sequentially, where each tree models the residual error of the previous ones, enabling strong non-linear regression capability.

• Adaptive Boosting (AB): A boosting algorithm that adaptively reweights samples to emphasize previously poorly predicted regions of the input space, improving robustness for heterogeneous sensor responses.

• Artificial Neural Network (ANN): A multilayer perceptron (MLP) with nonlinear activation functions, suitable for modelling multi-channel, low-frequency sensor signals with moderately complex temporal dynamics.

Before training, all feature dimensions were standardized to zero mean and unit variance based on the statistics of the training set. The dataset was partitioned at the window level into 70% training and 30% test subsets using a fixed random seed (42) to ensure reproducibility. For GB, we used regression trees with a maximum depth of 3, a learning rate of 0.05 and 200 estimators, which provided a good balance between bias and variance on the training data. For AB, shallow decision trees with a maximum depth of 3 were used as base learners, with 300 estimators and a learning rate of 0.1; this configuration was selected empirically as it yielded the lowest validation error without overfitting. The ANN was implemented as a multilayer perceptron with two hidden layers of 64 neurons each, rectified linear unit (ReLU) activations, and a linear output layer. The network was trained for up to 200 epochs with the Adam optimizer, a batch size of 32 and early stopping based on validation loss with a patience of 20 epochs. For each FSR channel, a separate model instance was trained using the same hyperparameters, and the model with the lowest validation error was retained for final testing.

A separate regressor from each family was trained for each FSR channel (r1–r6). This per-target configuration aligns with the sensor-specific organization of the dataset and allows each model to specialize in the force distribution characteristics of its respective plantar region.

Model performance was quantified using two established regression metrics:

• Mean Absolute Error (MAE): the average absolute deviation between predictions and reference FSR values (lower is better).

• Coefficient of Determination (R^2): the proportion of variance explained by the model (values closer to 1 indicate higher accuracy).

These metrics enable direct comparison with existing wearable insole studies, many of which report performance in the same format, thereby situating the proposed system within the broader context of plantar-force estimation research.

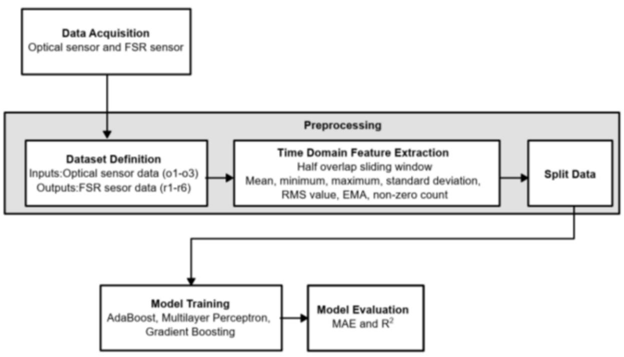

Figure 4: Machine Learning Workflow

3. RESULTS AND DISCUSSION

The regression results for plantar-force estimation are summarized in Table 1. Mean absolute error (MAE, in Newtons (N)) and coefficient of determination (R^2) are reported for each FSR channel (r1–r6, denoted as R1–R6 in the table) and each regression model (GB, AB, ANN). Across all sensors and models, R^2 ranges from 0.865 to 0.951 and MAE from 29.0 to 48.9 N. Given that the effective range of the FSRs is approximately 0–700 N, these errors correspond to about 5–7% of full scale, which is generally considered acceptable for plantar-force estimation and gait analysis applications. Overall, the models capture the mapping from optical features to reference forces with good fidelity.

Among the three model families, Adaptive Boosting (AB) provides the lowest average MAE across sensors (≈34–35 N) while maintaining a mean R^2 close to 0.90. AB attains the smallest MAE for r2–r6 and is the best overall performer for the distal sensors r5 and r6, where both MAE and R^2 are favorable. The artificial neural network (ANN) achieves the highest R^2 values for several proximal sensors (e.g. r1–r4), indicating that it captures a slightly larger fraction of variance, but its MAE is consistently higher than that of AB on the same channels. Gradient Boosting (GB) is competitive but rarely best-in-class; its performance typically lies between AB and ANN. These trends suggest that boosted-tree ensembles are particularly well suited to the moderately non-linear but piecewise-structured relationship between optical features and FSR responses, whereas the ANN can exploit stronger non-linearities at the expense of somewhat larger absolute errors.

For r1–r4—regions closer to the heel and midfoot—the ANN explains the variance very well (high R^2), while AB yields slightly smaller absolute errors. For r5 and r6—more distal regions under the forefoot—AB is clearly strongest in both MAE and R^2, and therefore represents the most robust choice when uniform performance across plantar regions is required. These differences are consistent with the local contact mechanics of the foot and with how the TPU optical fiber bends near each FSR location: regions with a more nearly linear relation between bending and force appear to favor boosted trees, whereas regions with more complex contact conditions benefit from the additional flexibility of the ANN. Figure 5 illustrates the regression behavior for sensor r1 using AB. The scatter points cluster closely around the identity line, in agreement with the R^2 value of 0.929 reported in Table 1. Three regimes can be distinguished qualitatively. First, a dense cluster near zero corresponds to swing phase or very low loading; this class imbalance explains why MAE remains moderate even when R^2 is high, as many samples are close to zero. Second, a broader spread in the mid-range (approximately 200–500 N) likely arises from small timing differences between optical and FSR responses within the sliding window, minor variations in optical micro-bending and local contact mechanics, and the inherent non-linearity of the optical–mechanical coupling. Third, a small number of outliers at the extremes reflect underestimation at high forces and overestimation at low forces, which may be linked to transient events, partial saturation of FSRs or short intervals in which the optical fiber experiences atypical bending. Despite these imperfections, the overall agreement between predicted and reference forces is good, reinforcing the quantitative results in Table 1.

From an application perspective, model selection depends on the desired trade-off between error magnitude and variance explained. If minimizing absolute error is the primary objective—for example, in real-time feedback or threshold-based monitoring—AB is the most consistent and reliable option, especially for r5 and r6, which are critical for propulsion. If maximizing explained variance and capturing subtle dynamics in specific regions is more important—for detailed biomechanical analysis, for instance—the ANN offers marginally higher R^2 for r1–r4. For a single model family to be deployed across all channels in a wearable device, AB provides the best balance between accuracy, robustness and implementation simplicity.

Table 1: Regression results for plantar-force estimation

Sensor	Algorithm	MAE (N)	R2
R1	GB	34.809	0.938
R1	AB	35.227	0.929
R1	ANN	38.219	0.951
R2	GB	39.344	0.865
R2	AB	29.024	0.868
R2	ANN	42.670	0.885
R3	GB	39.033	0.919
R3	AB	36.051	0.915
R3	ANN	37.766	0.931
R4	GB	44.136	0.898
R4	AB	35.498	0.910
R4	ANN	43.210	0.912
R5	GB	43.074	0.882

R5	AB	35.795	0.897
R5	ANN	46.403	0.879
R6	GB	38.423	0.885
R6	AB	33.414	0.896
R6	ANN	48.927	0.876

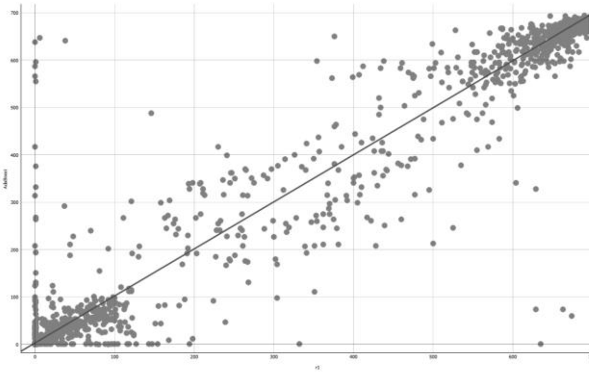

Figure 5: Regression plot for estimation of FSR sensor 1 (r1) with AB

3.1. Comparison with Related Works

This subsection positions the proposed system within the context of recent optical-fiber and machine-learning approaches for plantar-load sensing. Table 2 summarizes representative studies in terms of sensor technology, number of channels, target outputs, machine-learning usage and reported performance.

Leal-Junior et al. [9] presented a 3D-printed insole with 15 intensity-variation POF sensing points multiplexed on a single fiber by side-coupling. They estimated ground-reaction forces and centre of pressure with correlations exceeding 0.87 and reported R^2 values up to 0.97 across 20 subjects, together with body-mass estimation errors below 3.4%. Vilarinho et al. [13] embedded five FBGs in CYTOP POF for dynamic plantar-pressure monitoring and showed roughly two-fold higher sensitivity compared with silica FBGs, with root-mean-square errors around 160 kPa (below 5%) over gait cycles. Lakho et al. [14] used four silica FBGs placed under specific plantar landmarks to track posture-dependent load distributions after laboratory calibration, providing descriptive trends across postures rather than detailed quantitative error analysis. Jo and Park [12] implemented stretchable intensity-modulated optical fibers arranged in a grid within EVA foam to detect toe-walking; their system focuses on qualitative event detection (stance sequence and toe-walking patterns) rather than continuous force estimation. Mun and Choi [15] trained an LSTM network using nine Pedar-X pressure sensors as inputs to predict the remaining 90 sensors, achieving correlation coefficients around 0.98 and relative RMSE ≈ 7.9% on Pedar-X data; using a low-cost insole prototype, they reported correlations of 0.63–0.97 and relative RMSE ≈ 12.7 ± 7.4%. Compared with these works, the present prototype occupies a different point in the design space. The intensity-variation POF insole of Leal-Junior et al. [9] uses 15 side-coupled sensing regions and dedicated time-domain multiplexing to achieve high accuracy, but this design requires numerous channels and carefully engineered routing. The FBG-based insoles in [13, 14] rely on wavelength interrogation and specialized optical hardware; although they offer good sensitivity and “robustness, their optics and electronics are relatively complex and typically wired. The stretchable-fiber grid in [12] is well suited to robust event detection but does not provide continuous quantitative force outputs. The deep-learning approach in [15] predicts dense pressure maps from sparse resistive inputs using an LSTM, achieving strong correlations but at the cost of more sensors and heavier models.

In contrast, the system presented here intentionally keeps the hardware and signal chain minimal: three intensity-modulated TPU optical fibers (each with a single laser–LDR pair) and six reference FSRs are integrated into a 3D-printed insole, driven by a low-cost ESP32 microcontroller that streams data wirelessly at 22 Hz. No wavelength interrogation, multiplexing hardware or dense pressure arrays are required. Despite this simplicity and the use of non-anatomical, randomly routed fiber paths, the proposed method achieves R^2 values of approximately 0.88–0.95 and MAE of 5–7% of full FSR scale, comparable to the accuracy ranges reported for more complex systems. To the best of the authors’ knowledge, previous optical-fiber insole studies have not combined (i) highly irregular or random fiber layouts inside the insole, (ii) such a small number of optical channels and (iii) supervised machine learning that directly learns the mapping from optical signals to reference forces. This configuration demonstrates that machine learning can effectively compensate for irregular sensor geometries, enabling more flexible and manufacturable insole designs without sacrificing accuracy.

Table 2: Comparison with related works

Ref.	Sensor	Number of sensors	Target output	ML used	Key outputs /Performance metrics
[9]	Intensity-variation POF	15	GRF, CoP, pressure map	No	Corr. > 0.87; R^2 up to 0.97; body-mass error < 3.4 %
[13]	POFBG	5	Dynamic plantar pressure	No	Sensitivity ≈ 2× silica; RMSE ≈ 160 kPa (< 5 %)
[14]	Silica FBG	4	Posture-dependent pressure distribution	No	Descriptive trends across postures
[12]	Stretchable optical fiber	8	Toe-walking detection	No	Qualitative detection of stance sequence
[15]	Resistive pressure	9	Full pressure map estimation	LSTM	r = 0.98; rel. RMSE ≈ 7.9 % (Pedar-X); r = 0.63–0.97; rel. RMSE ≈ 12.7 ± 7.4 % (prototype)
Proposed method	TPU optical fiber + FSR	3 optical inputs; 6 FSR outputs	Estimate FSR forces from optical signals	AB, GB, shallow ANN	R^2 ≈ 0.88–0.95; overall MAE ≈ 29.0–48.9 N (≈5–7% of FSR full scale); for AB, MAE ≈ 29.0–36.1 N

4. CONCLUSION

This study demonstrates that randomly routed, flexible TPU optical fiber sensors can enable practical and accurate plantar-force estimation when combined with supervised machine learning. The insole integrates three TPU optical fiber lines and six reference FSRs within a 3D-printed TPU structure, read by an ESP32 microcontroller and streamed wirelessly at 22 Hz. Instead of relying on anatomically fixed sensor grids, the system uses a non-anatomical (random) optical layout and learns the mapping from optical intensity changes to FSR forces. With simple window-based time-domain features and standard regressors (GB, AB and a shallow ANN), the models achieve R^2 values between 0.865 and 0.951 and MAE values between 29.0 and 48.9 N, corresponding to approximately 4–7% of the FSR full scale; for the best family (AB), MAE is on the order of 4–5% of full scale. These results indicate that the optical signals carry sufficient information about local loading even without carefully designed sensor placement, and that machine learning can effectively compensate for irregular layouts while preserving accuracy levels comparable to more complex insole systems reported in the literature.

Among the tested models, Adaptive Boosting offers the lowest average MAE with robust R^2 across all sensors, making it a strong candidate for deployment as a single model family in wearable implementations. The ANN sometimes attains the highest R^2, particularly for heel and midfoot channels, suggesting an advantage in capturing more pronounced nonlinearities, while GB remains competitive but rarely superior. From a design perspective, the combination of low-cost components, minimal channel count (3 optical inputs, 6 reference FSR outputs), random fiber routing, wireless operation and lightweight models supports an alternative insole architecture: rather than enforcing anatomically precise placement or dense pressure arrays, the focus can shift to manufacturability, comfort and scalability, with the learning algorithm bridging the gap between irregular sensor geometry and clinically meaningful force estimates.

These findings should nonetheless be interpreted in light of several limitations. The current experiments were conducted with a single participant and one controlled walking condition (one-minute trials at 1 km/h), which is sufficient to establish feasibility but does not capture inter-subject variability or a wide spectrum of speeds, terrains and gait patterns. The FSRs are used as reference targets instead of a calibrated force platform or high-resolution in-shoe pressure system; nonlinearity, drift and hysteresis in the FSRs may therefore propagate into the learned models and the reported error metrics. The acquisition system operates at a sampling frequency of 22 Hz, chosen as a compromise between temporal resolution, wireless bandwidth and power consumption when streaming nine analog channels; at this low speed the models primarily capture quasi-static force envelopes rather than high-frequency impact transients. The modelling pipeline employs only basic time-domain features and a simple train–test split without explicit cross-validation or subject-independent testing, which may yield optimistic generalization estimates. Finally, intensity-based optical sensing remains sensitive to fiber routing, micro-bends, and long-term stability of the laser–fiber–receiver coupling, all of which may vary across users and over time.

Future work will address these issues systematically. On the experimental side, studies will be extended to larger and more diverse cohorts, with multiple walking and running speeds, additional tasks (e.g. turning, stair negotiation, uneven terrain) and varied footwear. Ground-truth forces and pressure distributions will be acquired using force plates and/or high-resolution pressure insoles to more rigorously quantify absolute errors. On the sensing side, improved fiber anchoring, protective coatings, and standardized coupling fixtures will be investigated to reduce drift and enhance repeatability, together with semi-random or algorithmically guided routing strategies that preserve manufacturability while enhancing sensitivity in key plantar regions. On the modelling side, richer temporal descriptors (lags, derivatives, short-term trends) and lightweight sequence models (temporal convolution, compact recurrent architectures) will be explored, along with k-fold and subject-wise cross-validation protocols to obtain more stringent estimates of generalization. Increasing the sampling rate to 50–100 Hz and combining it with enhanced temporal modelling is expected to reduce MAE by approximately 20–30%, targeting an error range of roughly 3–5% of full scale, comparable to that of more complex in-shoe systems with denser sensor arrays.

In summary, the results show that accurate multi-channel plantar-force estimation is attainable with a minimal, low-cost TPU optical fiber setup and a random sensor layout, provided that appropriate learning methods are applied. By simplifying hardware while maintaining competitive accuracy, the proposed approach opens a path toward scalable, customizable smart insoles that are easier to manufacture, fit and deploy for everyday gait monitoring, rehabilitation support and performance applications.

ACKNOWLEDGEMENTS

This study was supported by Pamukkale University Scientific Research Projects (BAP) Unit under project number 2022FEBE024. The walking experiments were conducted on a single healthy adult participant, author Hüseyin Öztürksoy. The protocol was non-invasive, did not involve any clinical intervention or collection of identifiable personal health data, and was limited to a short treadmill walking task while wearing the prototype insole. According to the institutional guidelines of Pamukkale University for engineering feasibility studies, this type of self-experiment is exempt from formal ethics committee review. The participant provided informed consent for data collection and publication.

REFERENCES

1. Seçkin, A.Ç., Ateş, B., and Seçkin, M., 'Review on Wearable Technology in Sports: Concepts, Challenges and Opportunities', Applied Sciences, Vol. 13, Issue 18, Pages 10399, 2023.

2. Dong, T., Wang, J., Chen, Y., Liu, L., You, H., and Li, T., 'Research Progress on Flexible 3-D Force Sensors: A Review', IEEE Sensors Journal, Vol. 24, Issue 10, Pages 15706–15726, 2024.

3. Peng, S., Hassan, H., Rosseel, S., Matricali, G.A., Deschamps, K., Vandeginste, V., and Hallez, H., 'Recent Advances in 3-D Printed, Wearable Pressure Sensors for Plantar Pressure Monitoring: A Review', IEEE Sensors Journal, Vol. 24, Issue 21, Pages 33903–33921, 2024.

4. Gan, J., Yang, A., Guo, Q., and Yang, Z., 'Flexible Optical Fiber Sensing: Materials, Methodologies, and Applications', Advanced Devices & Instrumentation, Vol. 5, Pages 0046, 2024.

5. Leal-Junior, A.G., Diaz, C.A.R., Avellar, L.M., Pontes, M.J., Marques, C., and Frizera, A., 'Polymer Optical Fiber Sensors in Healthcare Applications: A Comprehensive Review', Sensors, Vol. 19, Issue 14, Pages 3156, 2019.

6. Chuter, V.H., Spink, M.J., David, M., Lanting, S., and Searle, A., 'Clinical foot measurements as a proxy for plantar pressure testing in people with diabetes', Journal of Foot and Ankle Research, Vol. 14, Issue 1, Pages 56, 2021.

7. Saha, D., Prabhu, S., Thapliyal, A., and Pai, M.M.M., 'Analysis of Plantar Pressure to detect Foot Abnormalities among various subjects', 2023 International Conference on Advances in Intelligent Computing and Applications (AICAPS), 2023 International Conference on Advances in Intelligent Computing and Applications (AICAPS), Pages 1–6, 2023.

8. Castro-Martins, P., Marques, A., Coelho, L., Vaz, M., and Baptista, J.S., 'In-shoe plantar pressure measurement technologies for the diabetic foot: A systematic review', Heliyon, Vol. 10, Issue 9, 2024.

9. Leal-Junior, A.G., Díaz, C.R., Marques, C., Pontes, M.J., and Frizera, A., '3D-printed POF insole: Development and applications of a low-cost, highly customizable device for plantar pressure and ground reaction forces monitoring', Optics & Laser Technology, Vol. 116, Pages 256–264, 2019.

10. Jo, J., and Park, H., 'Fiber Optic-embedded Gait-Tracking Insole for Detection of Toe-Walking in Children with Autism Spectrum Disorder', International Textile and Apparel Association Annual Conference Proceedings, 2022

11. Noh, Y., Sareh, S., Würdemann, H., Liu, H., Back, J., Housden, J., Rhode, K., and Althoefer, K., 'Three-Axis Fiber-Optic Body Force Sensor for Flexible Manipulators', IEEE Sensors Journal, Vol. 16, Issue 6, Pages 1641–1651, 2016.

12. Mondal, B., and Mandal, D., 'Geometry-modulated all organic 3D printed smart PLA fibers for flextension amplified giant mechanical energy harvesting and Machine learning assisted pressure mapping', Chemical Engineering Journal, Vol. 496, Pages 154281, 2024.

13. Vilarinho, D., Theodosiou, A., Leitão, C., Leal-Junior, A.G., Domingues, M.D.F., Kalli, K., André, P., Antunes, P., and Marques, C., 'POFBG-Embedded Cork Insole for Plantar Pressure Monitoring', Sensors, Vol. 17, Issue 12, Pages 2924, 2017.

14. Lakho, R.A., Yi-Fan, Z., Jin-Hua, J., Cheng-Yu, H., and Ahmed Abro, Z., 'A smart insole for monitoring plantar pressure based on the fiber Bragg grating sensing technique', Textile Research Journal, Vol. 89, Issue 17, Pages 3433–3446, 2019.

15. Mun, F., and Choi, A., 'Deep learning approach to estimate foot pressure distribution in walking with application for a cost-effective insole system', Journal of NeuroEngineering and Rehabilitation, Vol. 19, Issue 1, Pages 4, 2022.